DNA Repair 22 (2014) 153–164

Contents lists available at ScienceDirect

DNA Repair

journal homepage: www.elsevier.com/locate/dnarepair

High levels of BRC4 induced by a Tet-On 3G system suppress DNA repair and impair cell proliferation in vertebrate cells

Takuya Abe*, Dana Branzei*

IFOM, The FIRC Institute for Molecular Oncology Foundation, IFOM-IEO Campus, Via Adamello 16, 20139 Milan, Italy

ARTICLE INFO

Article history:
Received 9 July 2014
Received in revised form 1 August 2014
Accepted 21 August 2014
Available online 16 September 2014

Keywords:
Homologous recombination
RAD51
BRC4
BRCA2
Tet-On system
DT40 cells

ABSTRACT

Transient induction or suppression of target genes is useful to study the function of toxic or essential genes in cells. Here we apply a Tet-On 3G system to DT40 lymphoma B cell lines, validating it for three different genes. Using this tool, we then show that overexpression of the chicken *BRC4* repeat of the tumor suppressor *BRCA2* impairs cell proliferation and induces chromosomal breaks. Mechanistically, high levels of BRC4 suppress double strand break-induced homologous recombination, inhibit the formation of RAD51 recombination repair foci, reduce cellular resistance to DNA damaging agents and induce a G2 damage checkpoint-mediated cell-cycle arrest. The above phenotypes are mediated by BRC4 capability to bind and inhibit RAD51. The toxicity associated with *BRC4* overexpression is exacerbated by chemotherapeutic agents and reversed by *RAD51* overexpression, but it is neither aggravated nor suppressed by a deficit in the non-homologous end-joining pathway of double strand break repair. We further find that the endogenous BRCA2 mediates the cytotoxicity associated with *BRC4* induction, thus underscoring the possibility that BRC4 or other domains of BRCA2 cooperate with ectopic BRC4 in regulating repair activities or mitotic cell division. In all, the results demonstrate the utility of the Tet-On 3G system in DT40 research and underpin a model in which BRC4 role on cell proliferation and chromosome repair arises primarily from its suppressive role on RAD51 functions.

1. Introduction

Homologous recombination (HR) is essential for genome integrity as it protects against DNA lesions derived from both endogenous and exogenous sources. The recombination mediator RAD51, the homologue of yeast Rad51 and bacterial RecA, plays central roles in HR in all organisms studied to date. Its coating of single strand (ss) DNA, exposed at stalled replication forks or formed during resection of double strand breaks (DSBs), leads to the formation of a nucleoprotein filament that can invade a homologous duplex to promote DNA repair [1]. HR and RAD51 activities need to be tightly regulated in the cell: low levels of RAD51 cause chromosome breakage and reduced cell proliferation, but increased levels of RAD51 also lead to genomic rearrangements by its ability to induce aberrant or ectopic recombination with repeats or non-homologous chromosomes [2,3].

The BRCA2 tumor suppressor, which is associated with a substantial fraction of familial breast cancers, participates in DNA recombination and repair processes, and is well known for its recombination mediator function [4]. Critical for the function of BRCA2 is its interaction with RAD51 [4–8], which is largely mediated by the eight internal BRC repeats contained in BRCA2 [9,10]. Of these BRC repeats, BRC3 and BRC4 have been thoroughly characterized biochemically. They bind to RAD51 [5,7,8,10,11], and whereas low concentrations of BRC4 and BRC3 enhance RAD51 binding to ssDNA and stimulate RAD51-mediated strand exchange [10,12,13], high concentrations of BRC4 and BRC3 disrupt RAD51 filament formation [6,11,12]. Consistent with these *in vitro* biochemical observations, both *BRCA2* knockout cells and *BRC4* overexpressing cells are defective in RAD51 foci formation and HR repair [7,8,14,15].

In this study, we examined the function of BRC4 on HR by conditionally overexpressing *BRC4* in chicken DT40 cells using a tetracycline-inducible Tet-On 3G system. The Tet-On system is especially useful when applied to cell lines in which the transfection efficiency of expression plasmids is low, as is the case of nerve and lymphocyte cell lines. While the bursal DT40 cell line has multiple valuable features for research [16], the transfection efficiency of expression plasmids is usually very low. Here, we employed a recently developed Tet-On 3G system and applied it to *p53*, presupposed to induce apoptosis-mediated cell cycle arrest, and to

* Corresponding authors. Tel.: +39 02 574 303 259.
E-mail addresses: takuya.abe@ifom.eu (T. Abe), dana.branzei@ifom.eu (D. Branzei).

http://dx.doi.org/10.1016/j.dnarep.2014.08.003

Table 1
Cell lines used in this study.

Genotype	Selective marker	Reference
WT CL18		[16]
WT + *DR-GFP* + I-*Sce*I (Tet-On)	Puro/Neo	This study
WT + *DR-GFP* + I-*Sce*I and *BRC4* (Tet-On)	Puro/Neo/Bsr	This study
WT + *BRC4* (Tet-On)	Neo	This study
WT + *BRC4 A1504S* (Tet-On)	Bsr	This study
WT + *BRC4* (Tet-On) + *hsRAD51*	Neo/Bsr	This study
BRCA2$^{+/-}$	Bsr/Puro	[15]
BRCA2$^{+/-}$ + *BRC4* (Tet-On)	Bsr/Puro/Neo	This study
XRCC4$^{/-}$ + *DR-GFP* + I-*Sce*I (Tet-On)	Neo/Puro/His	This study
XRCC4$^{/-}$ + *BRC4* (Tet-On)	Puro/Neo/His	This study
XRCC3$^{-/-}$	Bsr/His	[17]
RAD51$^{-/-}$ + *hsRAD51*	Puro/Bsr/Neo/Hyg	[18]

BRC4 and I-*Sce*I to study their effect on recombinational repair. In all cases, we achieved high enough induction to cause cell death in the presence of doxycycline (Dox) and detected no leaky expression in its absence, thus demonstrating the general utility of the Tet-On 3G system in DT40 research for studies of conditional or transient induction of genes.

Using these new tools, here we report that conditional induction of the *BRC4* repeat of *BRCA2* impairs cell proliferation of chicken DT40 cells by inducing a G2 damage checkpoint-mediated arrest and an accumulation of chromosome gaps and breaks. *BRC4* induction suppresses HR and reduces cellular resistance to DNA damaging agents. These effects are mediated by BRC4 binding to RAD51 and counteracted by *RAD51* overexpression. Non-homologous end joining (NHEJ) was not responsible for the phenotypes associated with *BRC4* induction, nor was required to sustain viability in these cells, indicating that NHEJ is actively suppressed in G2 even when the HR pathway is defective. Moreover, we find that endogenous BRCA2 is required for BRC4 cytotoxicity, suggesting a possible crosstalk between BRC4 and other BRCA2 domains in regulating DNA repair or mitotic cell division.

2. Materials and methods

2.1. Cell culture techniques and cell viability/drug sensitivity assays

Cells were cultured at 39.5 °C in D-MEM/F-12 medium (Gibco) supplemented with 10% fetal bovine serum, 2% chicken serum (Sigma), Penicillin/Streptomycin mix, and 10 μM 2-mercaptoethanol (Gibco) in the presence or absence of 1 μg/ml Dox. The cell lines used in this study are shown in Table 1. To plot growth curves, each cell line was cultured in three different wells of 24 well-plates and passaged every 12 h. Cell number was determined by flow cytometry using plastic microbeads (07313-5; Polysciences). Cell solutions were mixed with the plastic microbead suspension at a ratio of 10:1, and viable cells determined by forward scatter and side scatter were counted when a given number of microbeads were detected by flow cytometry. mCherry positive cells were detected by FL2-H as shown in Fig. 2A.

2.2. Plasmid construction and transfection

Tet-On® 3G Inducible Expression System (with mCherry) containing pTRE3G-mCherry and pCMV-Tet3G vectors was purchased from Clontech. Chicken *BRC4* cDNA was prepared by reverse transcription PCR using 5′-GGAACTTATCTGACTGGTTTCTGTACTGC-3′ (sense) and 5′-ATCTGCATCACAATGAGCAGTACTGTCC-3′ (antisense) primers. The *Nde*I site and *NLS* to its N-terminal end and a *FLAG* tag and *Bam*HI site to its C-terminal end were added by PCR using 5′-CATATGCCAAA GAAGAAACGCAAGGTGGGAACTTATCTGACTGGTTTCTGTACTGC-3′ (sense) and 5′-GGATCCTTACTTGTCGTCATCGTCTTTGTAGTCTGCATC ACAATGAGCAGTACTGTCC-3′ (antisense) primers. *BRC4* was then cloned into the pTRE3G-mCherry vector. The amino acid sequence of BRC4 used in this study except for NLS and FLAG is GTYLTGFCTASGKKITIADGFLAKAEEFFSENNVDL-GKDDNDCFEDCLRKCNKSYVKDRDLCMDSTAHCDAD (amino acid residues 1495–1566 of chicken BRCA2). Similarly, *p53* cDNA was amplified using 5′-GAATTCCGAACGGCGGCGGCGGC-3′ (sense) and 5′-GCTGAAGGGAAAGGGGGCGTGGTAAAGG-3′ (antisense) primers, then an *Nde*I site to its N-terminal and a *FLAG* tag and *Bam*HI site to its C-terminal were added by PCR using 5′-CATATGGCGGAGGAGATGGAACCATTGCTGG-3′ (sense) and 5′-GGATCCTTACTTGTCGTCATCGTCTTTGTAGTCCATGTCCGAGCCTTTTT GCAGCAGTTTCTTCC-3′ (antisense) primers. After cloning *p53* into the pTRE3G-mCherry vector, the premature stop codon of *p53* was corrected by site directed mutagenesis using 5′-CTGTTGGGGCGGCGCTGCTTCGAGGTGCGC-3′ (sense) and 5′-GCGCACCTCGAAGCAGCGCCGCCCCAACAG-3′ (antisense) primers. I-*Sce*I was tagged with an *Nde*I site N-terminally and a *FLAG* and *Bam*HI site C-terminally by PCR using 5′-CATATGGGATCAAGATCGCCAAAAAAGAAGAG-3′ (sense) and 5′-GGATCCTTACTTGTCGTCATCGTCTTTGTAGTCCATTTTCAGGAAAGTTT CGGAGGAGATAGTG-3′ (antisense) primers, and cloned into the pTRE3G-mCherry vector. These expression vectors were transfected to DT40 cells with pCMV-Tet3G vectors in the ratio (6:1), and cells expressing the target genes in the presence of Dox were selected. *BRC4-A1504S* cells were obtained by transfecting an identical *BRC4* construct containing the A1504S mutation engineered by QuickChange Site Directed Mutagenesis using 5′-CTGACTGGTTTCTGTACTTCTAGTGGCAAG-3′ (sense) and 5′-CTTGCCACTAGAAGTACAGAAACCAGTCAG-3′ (antisense) primers. *hsRAD51* overexpression clones were obtained as previously described [17]. The *XRCC4* knockout constructs are previously reported [19]. Briefly, the 110–165 amino acid fragment of XRCC4 (full length 283 amino acids) was replaced by drug resistance marker genes.

2.3. DNA fragmentation assay

DNA fragmentation assay was performed as previously described [19]. Cells were lysed, and genomic DNA was extracted using Easy DNA kit (Invitrogen) according to the manufacturer's protocol. DNA was quantified and 4 μg was electrophoresed in a 2% agarose gel containing ethidium bromide (0.5 μg/ml). DNA ladders were visualized under an ultraviolet light and photographed.

2.4. Western blotting

Western blotting were performed as previously described [19] using antibodies against MCM7 or RAD51 (Santa Cruz), α-tubulin or FLAG-M2 (Sigma), pCHK1 S345 (Cell Signaling), γ-H2AX (Millipore) followed by horseradish peroxidase-conjugated anti-rabbit, anti-rabbit, or anti-mouse IgG secondary antibody (Cell Signaling). Proteins were visualized using SuperSignal West Femto Maximum Sensitivity Substrate (Thermo Scientific).

2.5. Cell cycle analysis by flow cytometry

Flow cytometry was performed as previously described [18]. Cells were cultured in the presence of BrdU for 15 min, fixed in 70% ethanol, incubated with anti-BrdU antibody (BD Biosciences), and stained with FITC-conjugated anti-mouse IgG antibody (Sigma) and propidium iodide. For PI single staining analysis, cells were fixed in 70% ethanol and stained with propidium iodide.

2.6. mRNA isolation, reverse transcription and qPCR

Total RNA was isolated using TRIzol reagent (Invitrogen) and converted to cDNA with Superscript III (Invitrogen). The cDNA was amplified with GoTaq® qPCR Master Mix (Promega) and LightCycler® 480 system (Roche). Normalization of the amount of cDNA was done with *β-actin*. The primers used to amplify *BRC4* were 5′-CAATTGCTGATGGATTTTTGGC-3′ (sense) and 5′-GTCACGGTCTTTAACATAGC-3′ (antisense), and the primers used to amplify *β-actin* were 5′-CGTGCTGTGTTCCCATCTATCGTG-3′ (sense) and 5′-TACCTCTTTTGCTCTGGGCTTCATC-3′ (antisense).

2.7. Immunofluorescent visualization of subnuclear RAD51 foci formation

Immunocytochemical analysis was performed as described in [17]. Briefly, DT40 cells (10^5 cells) were treated with MMC (500 ng/ml) for 1 h, washed with warm medium 3 times and cultured for an additional 1 h at 39.5 °C. Cells were washed with PBS and spun onto Nunc® Lab-Tek® II Chamber Slide system by centrifugal attachment. Cells were fixed with 4% formaldehyde for 15 min at room temperature, and permeabilized with 0.5% triton/PBS. After blocking with 3% BSA, fixed cells were treated with RAD51 antibodies (1:500; Santa Cruz) followed by Alexa488-conjugated anti-rabbit IgG (1:100; Molecular Probes). In Fig. 8D and E, in order to detect RAD51 foci even in the presence of overexpressed *RAD51*, cells were treated with MMC for 6 h and pre-extracted by 0.1% triton/PBS for 3 min prior to fixation. At least 100 morphologically intact cells were examined. Cells with more than four brightly fluorescing foci were scored as positive.

3. Results

3.1. Establishment of the Tet-On 3G system in DT40 cells

To establish a good conditional expression system in DT40 cells, we applied the newly developed Tet-On 3G system in which both the tetracycline response elements present in the promoter [20] and the tetracycline-controlled transactivator protein [21] were optimized to achieve low background and high expression. We first examined the effects of expressing *p53*, thought to be inactive in DT40 cells [22]. *p53* expression is likely detrimental to DT40 cell proliferation by inducing apoptosis, similarly to its effect in other cancer cell lines [23]. To this purpose, we cloned amplified chicken *p53* using a DT40 cDNA library made by the reverse transcription reaction. Cloned *p53* was sequenced and we found mutations in both alleles of *p53* in DT40 cells. One is a premature stop codon mutation that leads to a C-terminal truncated protein (1–254 amino acids), the other is a deletion mutation in the C-terminus further accompanied by a frame shift (Supplementary Fig. 1). To obtain intact chicken *p53*, the premature stop codon of the first allele of *p53* was corrected by site directed mutagenesis and the new allele was cloned into the pTRE3G mCherry vector, which allows monitoring of the expression of target proteins by detecting the concurrently expressed mCherry. Wild-type (WT) DT40 cells were co-transfected with *p53*/TRE3G mCherry construct and the pCMV-Tet3G vector, which contains a Neo resistant marker, and several clones that expressed mCherry after Dox addition were selected. Expression of *p53*, induced by addition of Dox, immediately blocked cell growth (Fig. 1A) and led to apoptosis as detected by DNA ladder formation (Fig. 1B). In the absence of Dox, the cells containing Tet-On-*p53* grew as fast as WT (Fig. 1A). These results indicate that the Tet-On 3G system is proficient at inducing *p53* at levels high enough to kill DT40 cells. In addition, no detectable leaky expression of p53 in the absence of Dox was observed as assessed by examining protein levels by Western blotting (Fig. 1C).

3.2. Measurement of HR-dependent DSB repair using Tet-On 3G I-SceI system

By using a similar approach, we next expressed I-*Sce*I, a homing endonuclease commonly used in various reporter assay (such as DR-GFP) that are based on induced DSBs at I-*Sce*I sites [24]. Repair by HR restores a functional cassette, in this case GFP, the expression levels of which can be conveniently monitored *via* FACS. In these assays, I-*Sce*I is usually introduced by transfection. However, the transfection efficiency varies greatly with the cell line and the transfection procedure itself causes cytotoxicity. Furthermore, the expression levels of I-*Sce*I in each cell are not constant, being dependent on the level of transfected plasmids. To overcome these caveats, we applied the Tet-On 3G system described above also to I-*Sce*I. After transfection of 30 μg of I-*Sce*I/TRE3G mCherry vector together with 5 μg of pCMV-Tet3G vector to 10^7 of cells and following drug selection by G418, we got 22 drug resistance clones, 10 of which expressed mCherry after Dox addition. mCherry expression ratios of these clones were from 99.26% to 99.9%, 72 h after Dox addition. None of these clones displayed leaky expression monitored by mCherry in the absence of Dox. One clone out of the ten that expressed high levels of mCherry was picked up and further characterized phenotypically. In the absence of Dox, no cells expressing mCherry (or I-*Sce*I) could be detected (Fig. 2A). Addition of Dox, however, induced mCherry on 98.5% of living population within 48 h (Fig. 2A and B). mCherry induction was kept in 96.9% of living population even after 120 h (Fig. 2A and B). Expressed I-*Sce*I efficiently elicited recombination in the DR-GFP construct, making 3.7% of the living population GFP positive already after 48 h. The induction frequency is much higher than that induced by transient transfection using the Amaxa Nucleofector, so far thought to achieve maximum transfection efficiency in DT40 cells [24]. Notably, an advantage of the Tet-On 3G system is its ability to ensure consistent and continuous expression levels of I-*Sce*I, compared to the ones achieved by transient transfection [24]. Because the population of GFP positive cells increased gradually following I-*Sce*I induction (Fig. 2B), we concluded that most of DSBs are repaired without base pair change and therefore are likely re-cut by I-*Sce*I again. GFP positive population reached a plateau around 20%, 8 days after the addition of Dox (Fig. 2B). Likely, at this time, I-*Sce*I sites were either replaced by upstream donor sequences (20%) or mutated due to the DSB end processing (the rest of 80%). DSBs are generally repaired by two major pathways: NHEJ that ligates broken DNA ends with no regard for homology, and by homology-directed repair that relies on DSBs being processed to expose single strand ends, which can then either invade homologous double-stranded (ds) DNA, a process known as HR, or anneal with other homologous ssDNA, a process known as single-strand annealing [1]. The I-*Sce*I -induced recombination frequency is highly up-regulated in NHEJ-deficient mutants, suggesting that the DSBs induced by I-*Sce*I are predominantly repaired by NHEJ in DT40 cells, and in the absence of NHEJ activity, they are funneled toward HR [25].

To recapitulate this feature in our system, we expressed I-*Sce*I in the NHEJ mutant *XRCC4*$^{-/-}$ containing the DR-GFP reporter assay. NHEJ depends on the LigaseIV/XRCC4/XLF ligation complex activity [26]. We note that chicken *XRCC4* is located on chromosome *Z* and therefore only one targeting disruption is enough to obtain *XRCC4* deficient cell lines [19]. In line with the notion above on the predominance of NHEJ in repairing I-*Sce*I -induced DSBs, *XRCC4*$^{-/-}$ cells showed highly elevated levels of HR, with about 25% of total cell population being GFP-positive 48 h after I-*Sce*I induction as compared to about 5% in WT cells (Fig. 2C). Altogether, these results

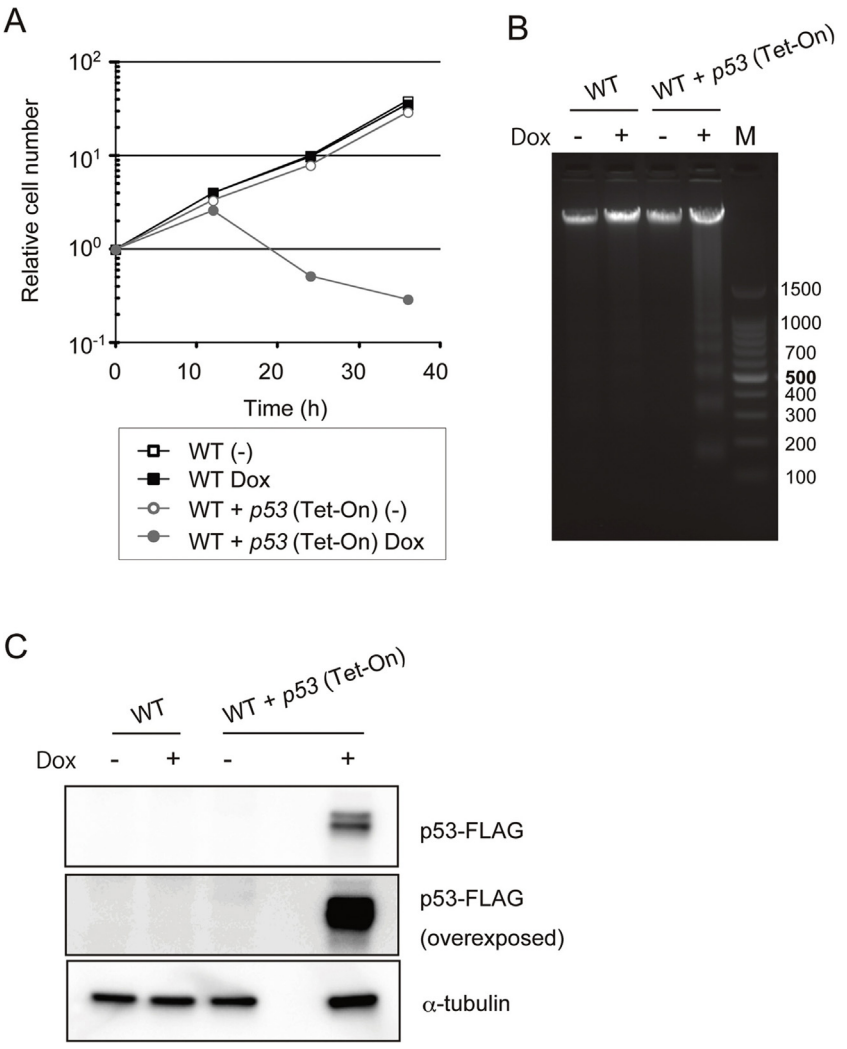

Fig. 1. Cellular effects associated with inducible *p53* in chicken DT40 cells. (A) Growth curves. WT or WT + *p53* (Tet-On) cells (1×10^5) were inoculated in 1 ml of medium and passaged every 12 h. Dox was added at time 0. (B) DNA fragmentation assay. Genomic DNA was prepared and subjected to agarose gel electrophoresis. DNA ladders were detected by staining with 0.5 μg/ml ethidium bromide. M indicates the 100 bp DNA Ladder marker. (C) Monitoring of p53-FLAG. Whole cell lysates were prepared from cells cultured in the absence or the presence of Dox for 12 h. p53-FLAG and α-tubulin (loading control) were detected by Western blotting.

indicate that the Tet-On 3G system is a powerful tool that can be successfully applied to induce the expression of various types of genes without leaky expression in the absence of Dox.

3.3. Characterization of the cytotoxic effect of the BRC4 peptide

With the purpose of examining *in vivo* the effects of the BRC repeats of BRCA2 on DNA repair/recombination and cell viability, we next applied the Tet-On 3G system to *BRC4*. The amino acid sequence identity of chicken BRCA2 with that of the human homolog is 40%, and while human BRCA2 has eight BRC repeats, chicken BRCA2 contains only the BRC-1, 2, 4, 7, and 8 repeats [27]. Because BRC3 and BRC4 repeats in human were characterized biochemically [5,7,8,10,11], but only BRC4 is conserved in chicken, we chose BRC4 for our study. To this end, the BRC4 peptide was tagged with the SV40 nuclear localization signal (NLS) in its N-terminus and with FLAG in its C-terminus, and expressed by the Tet-On 3G System. After transfection, several clones expressing *BRC4–FLAG* were obtained. Hereafter, we refer to these WT cells containing the *NLS–BRC4–FLAG* (Tet-On) construct as '*BRC4*' cells. Dox addition efficiently induced mRNA and protein of *BRC4* cells (Fig. 3A and B). The expression level of *BRC4* mRNA at 12 h after addition of Dox is 500 to 1000-fold higher than the one observed without Dox (Fig. 3A). We then examined the growth curve of *BRC4* cells and observed that *BRC4* induction severely blocked cell growth already after one cell-cycle (Fig. 3C). If toxic proteins such as BRC4 are induced over a long time, the rate of Dox resistant population appears increased because of the ensuing cell death (Fig. 3B, 48 h time point). To eliminate the Dox resistant population from our analysis, we repeated the experiment counting the number of mCherry expressing cells, which should also express BRC4 peptide simultaneously, and found that BRC4 expressing cells clearly stopped growing (Fig. 3D).

In addition to cytotoxicity, expression of *BRC4* also induced a large number of chromosomal aberrations of both gap and break types (Fig. 3E). This phenotype is reminiscent of the chromosomal aberrations accumulating upon inhibition of RAD51 in vertebrate and murine cells [18,28], although no major effects on RAD51 levels were observed upon *BRC4* induction (data not shown and see below). DT40 cells knocked out for the essential *RAD51* gene, but expressing the *Homo sapiens RAD51* transgene (*hsRAD51*) under the control of a Tet-repressible promoter, showed a similar pattern of chromosomal aberrations with the one observed upon *BRC4* overexpression (Fig. 3E) and [18]). Thus, *BRC4* induction leads to cytotoxicity that is associated with chromosome aberrations.

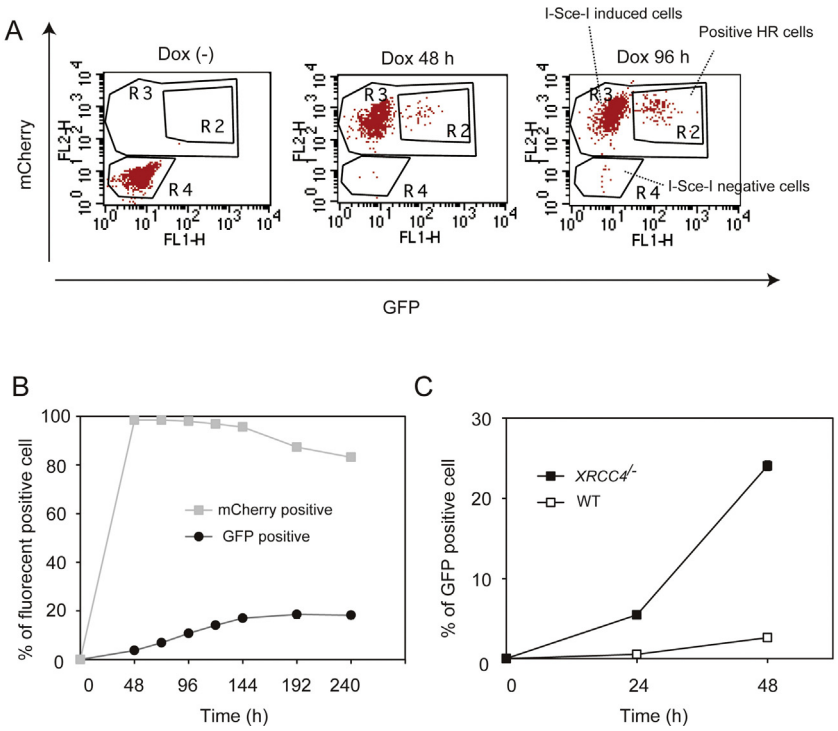

Fig. 2. Measurement of homologous recombination-dependent DSB repair. (A) WT + I-*Sce*I (Tet-On) cells containing the DR-GFP construct were incubated with Dox. mCherry and GFP expressing fractions were measured at the indicated time points. The vertical axis represents the expression level of mCherry and horizontal axis represents the expression level of GFP. R2, R3 and R4 indicate cells that underwent recombination, I-*Sce*I -induced cells and I-*Sce*I negative cells, respectively. (B) The percentage of the cell population expressing mCherry and GFP are plotted.

3.4. Characterization of the recombination and proliferation defects of BRC4 cells

BRC4 binds RAD51, inhibits its polymerization and suppresses HR [6,10]. To address whether inhibition of HR underlies the cytotoxicity associated with *BRC4* overexpression, we examined the effect of *BRC4* overexpression on I-*Sce*I -induced HR. To this end, we constructed cell lines co-expressing I-*Sce*I and *BRC4*. The HR frequency – assessed as GFP positive cells – was reduced almost by half in *BRC4* cells (Fig. 4A). In addition, *BRC4* induction also suppressed RAD51 foci formation both in unperturbed conditions or mitomycin C (MMC)-treated cells (Fig. 4B). Together, these results indicate that *BRC4* overexpression suppresses HR. To address if cell-cycle arrest underlies the cytotoxicity associated with *BRC4* overexpression, we monitored the cell cycle distribution by FACS analysis using the Bromodeoxyuridine (BrdU) antibody and propidium iodide (PI). *BRC4* cells showed a prominent G2/M arrest 12 h after Dox addition, with the percentage of subG1 population increasing at later time points (Fig. 4C). To understand whether *BRC4* cells arrested in the G2 phase of the cell cycle because of damage checkpoint activation or rather accumulated in M phase, *BRC4* cells were incubated with caffeine, an ATM/ATR inhibitor, 12 h after Dox addition. The G2/M arrest associated with *BRC4* overexpression was suppressed by caffeine addition (Fig. 4D), indicating that the *BRC4*-induced cell cycle arrest involved the G2/M checkpoint. We further monitored which branch of the damage checkpoint is induced upon *BRC4* overexpression. BRC4 did not cause ATR-dependent CHK1 phosphorylation, but induced ATM-dependent γ-H2AX phosphorylation [29] (Fig. 4E). These results indicate that BRC4 mainly creates DSBs in G2 without prior activation of the replication checkpoint, and that the accumulation of chromosomal breaks and gaps (see Fig. 3E) triggers ATM-mediated arrest in the G2 phase of the cell cycle.

3.5. BRC4 cytotoxicity is dependent on the amount of BRCA2

The role of BRCA2 in HR is crucial and very complex. BRCA2 does not simply stimulate RAD51 binding to DNA, but modulates the DNA binding affinity of RAD51 based on the structural characteristics of DNA [10]. In addition, by keeping RAD51 in a minimal oligomeric state, the C-terminal domain of BRCA2 also impinges on RAD51 ability to assemble nucleofilaments required to initiate HR strand exchange [30–33]. Furthermore, while *RAD51* overexpression compensates the deficiency in *RAD51* paralogs and *BRCA1* in terms of cellular sensitivity to cisplatin (CDDP) and MMC [17,34], it negatively affects cell growth and aggravates the hypersensitivity of *BRCA2*$^{tr/-}$ cells (BRC3 truncated BRCA2 mutant) to genotoxic agents [35]. These observations were interpreted as to indicate that BRCA2 has a role in suppressing "inappropriate" binding of RAD51 to DNA, whereas RAD51 paralogs and BRCA1 simply facilitate RAD51 polymerization. This idea, together with the effects observed following *BRC4* induction (Fig. 3), made us hypothesize that endogenous BRCA2 might also suppress RAD51 function through its BRC repeats and/or C-terminal domain or that the observed cytotoxicity associated with *BRC4* induction might be dependent on the presence of other BRC repeats or the C-terminus of BRCA2, proposed to play a regulatory role in BRC repeat-mediated RAD51 nucleofilament disassembly [31,32] or formation [33].

To test the above hypotheses, we introduced *BRC4* into *BRCA2*$^{-/+}$ heterozygous cells as *BRCA2*$^{-/-}$ cells are very slow growing [15], making it difficult to evaluate the cytotoxic effects associated with BRC4. Quantitative real time PCR revealed that two individual clones of *BRCA2*$^{-/+}$ *BRC4* cells expressed about half the level of *BRC4* mRNA in the absence of Dox (Fig. 5A), indicating that both alleles of *BRCA2* are equally active in DT40 cells. In the presence of Dox, comparable levels of *BRC4* mRNA and protein were induced in *BRCA2*$^{-/+}$

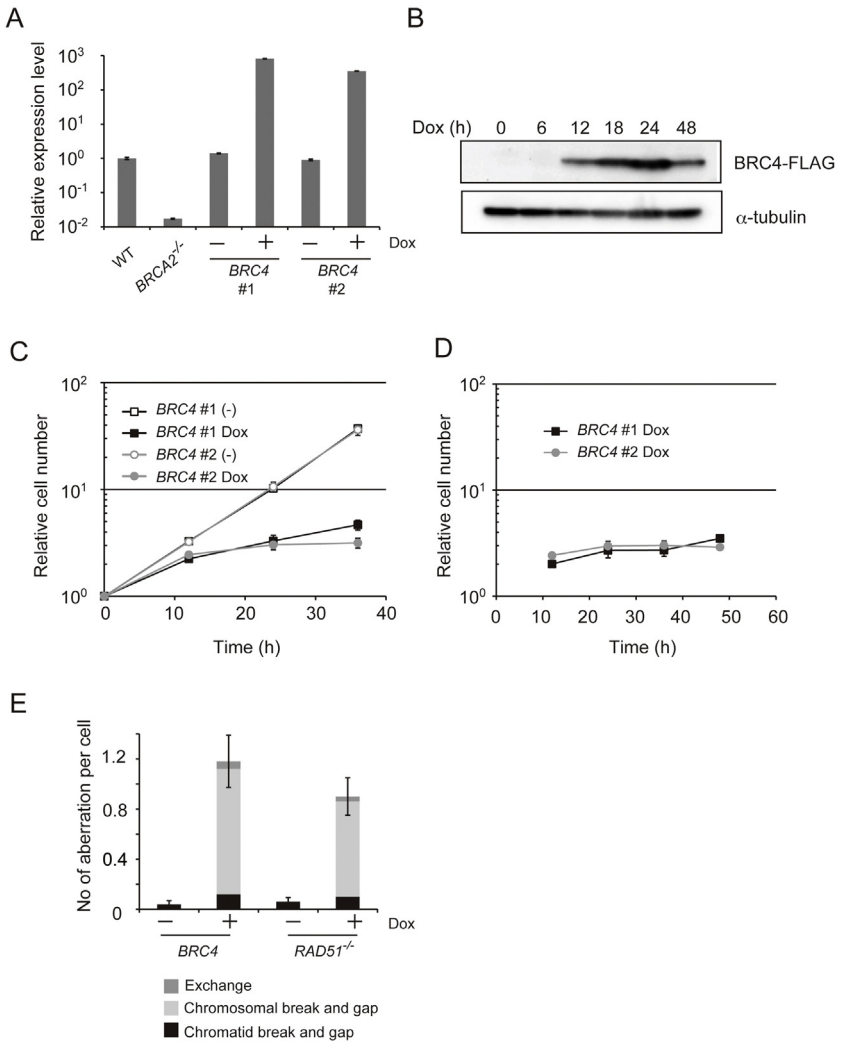

Fig. 3. High levels of BRC4 cause cytotoxicity. (A) Relative *BRC4* expression level measured by quantitative polymerase chain reaction (qPCR). WT, *BRCA2*$^{-/-}$ (negative control), and individually obtained 2 clones of *BRC4* cells (WT + *BRC4* (Tet-On) cells) were incubated in the presence or absence of Dox for 12 h when RNA was isolated and converted to cDNA. The cDNA was amplified with GoTaq® qPCR Master Mix. (B) Expression of the BRC4–FLAG peptide. Whole cell lysates were prepared from *BRC4* #1 cells cultured in the presence of Dox for the indicated times. BRC4–FLAG and α-tubulin (loading control) were detected by Western blotting. (C) Growth curves. Individually obtained 2 clones of *BRC4* cells (1×10^5) were inoculated in 1 ml of medium and passaged every 12 h. Dox was added at time 0. (D) Growth curves of mCherry positive cells. The number of cells expressing mCherry was counted every 12 h. (E) Number of chromosomal aberrations in *RAD51*$^{-/-}$ cells expressing *hsRAD51* from a Tet-inducible promoter and in *BRC4* cells after treatment with Dox for 18 h (*RAD51*$^{-/-}$ + *hsRAD51* cells) or for 24 h (*BRC4* cells).

BRC4 cells and *BRC4* cells (Fig. 5A and B, 24 h). Notably however, *BRCA2*$^{-/+}$ *BRC4* cells grew much better than *BRC4* cells in the presence of Dox (Fig. 5C). By eliminating the mCherry negative fraction (and therefore the Dox resistant population), the difference in growth became even more prominent (Fig. 5D). The chromosomal breaks/gaps associated with *BRC4* induction were also reduced in *BRCA2*$^{-/+}$ cells (Fig. 5E). These results demonstrate that endogenous BRCA2 contributes to BRC4 cytotoxicity, most likely by suppressing RAD51 polymerization or RAD51 nuclear filament formation.

3.6. *BRC4* cytotoxicity is independent of the NHEJ pathway

NHEJ acts by joining, often in an error-prone manner, the two ends of a DSB through the activation of the LigaseIV/XRCC4/XLF ligation complex [26]. We asked if BRC4-induced DNA damage/cytotoxicity, which appeared to be related to disruption of RAD51 and therefore to HR activity (Figs. 3C–E and 4A and B), is mediated by NHEJ. To address this question, we disrupted the *XRCC4* gene, an essential co-factor of LigaseIV, in *BRC4* cells. Differently from *BRCA2*$^{+/-}$ *BRC4* cells (see Fig. 5), *XRCC4*$^{-/-}$ *BRC4* cells were indistinguishable from *BRC4* cells as assessed by cell growth and chromosomal aberration phenotypes (Fig. 6A and B). These results indicate that NHEJ is neither involved in repairing the DNA damage associated with high levels of BRC4 (in which case *XRCC4*$^{-/-}$ *BRC4* cells are expected to have more severe phenotypes than *BRC4* cells) nor responsible for the cytotoxicity and chromosomal aberrations observed in *BRC4* cells (in which case *XRCC4*$^{-/-}$ *BRC4* cells would be expected to have alleviated phenotypes).

3.7. *BRC4* cytotoxicity is dependent on the RAD51 amount

In vitro and structural studies have shown the highly selective binding of BRC4 peptide to RAD51 [6,8]. To address the selectivity of BRC4 for RAD51 *in vivo* and assess if this accounts for its cytotoxicity (Fig. 3) and suppressive effect on HR (Fig. 4), we overexpressed *hsRAD51* in *BRC4* cells (described as *BRC4* + *hsRAD51*) (Fig. 7A). In contrast to *BRCA2* deficient cells, whose growth rate

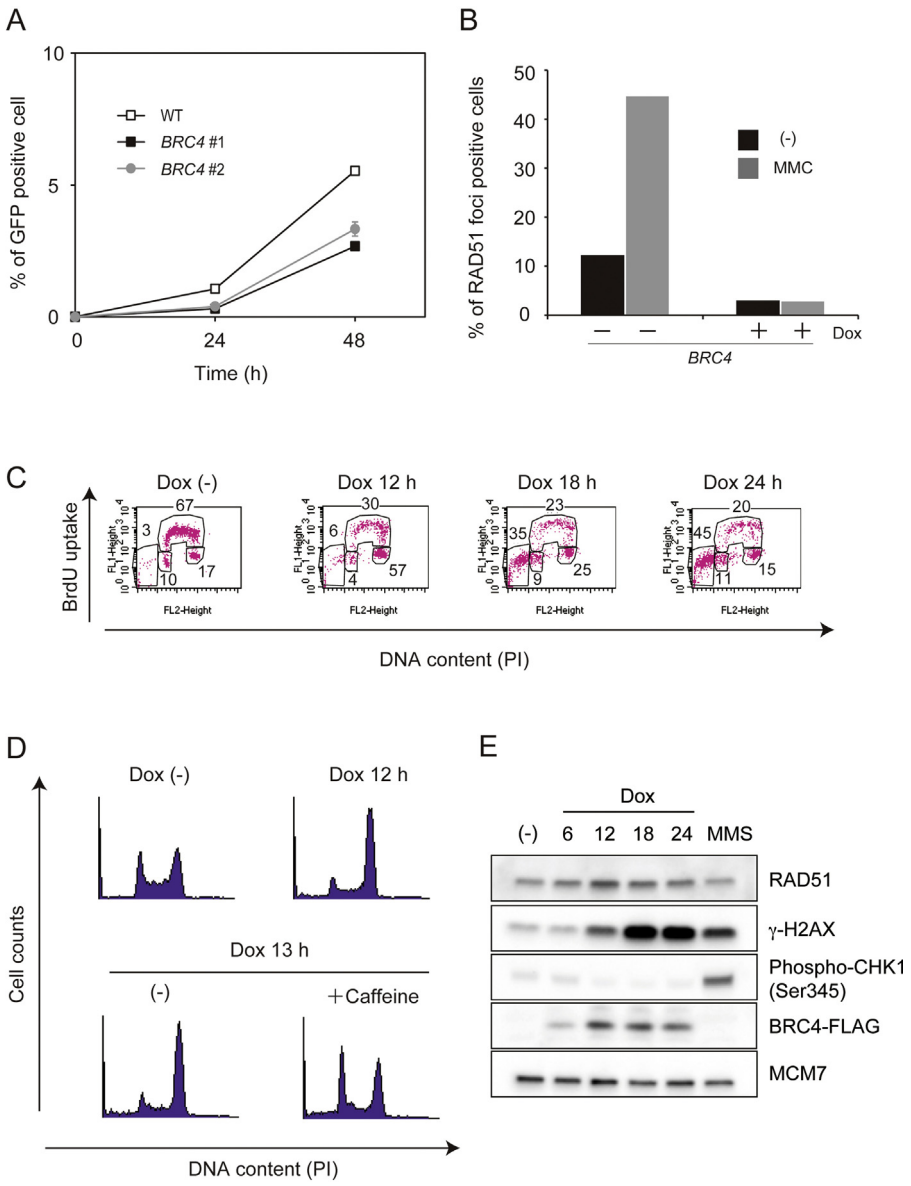

Fig. 4. BRC4 suppresses homologous recombination and activates the G2/M checkpoint, but not the ATR replication checkpoint. (A) Homologous recombination (HR) repair assay using the I-*Sce*I induced DSB formation at the DR-GFP reporter (see Fig. 2). Percentage of cells that underwent HR (measured as cells expressing GFP) is plotted. (B) Rad51 focus formation. *BRC4* cells were incubated in the presence or absence of Dox for 18 h. Cells were exposed to 500 ng/ml of MMC for 1 h, then washed, and sampled after 1 h. At least 100 cells were scored for each preparation. Identical trends were observed in two independent experiments. (C) Cell cycle distribution of *BRC4* cells. Cells were cultured in the presence of Dox for the indicated times, pulse-labeled with BrdU for 15 min, and harvested. The cells were stained with FITC anti-BrdU to detect BrdU uptake and with propidium iodide (PI) to detect DNA. The vertical axis represents BrdU uptake and horizontal axis represents total DNA. The gates represent SubG1 (apoptotic cells), G1, S and G2/M phase from left to right, in this order. Numbers show the percentage of cells falling in each gate. (D) *BRC4* cells were cultured in the presence of Dox for 12 h, further cultured in the presence or absence of Caffeine for 1 h and used for FACS analysis. (E) *BRC4* cells were cultured in the presence of Dox for indicated times and whole cell lysates were prepared from each time points. RAD51, γ-H2AX, pCHK1 S345, BRC4–FLAG and MCM7 (loading control) were detected by Western blotting.

and cisplatin sensitivity are aggravated by *RAD51* overexpression [35], excess amount of RAD51 completely rescued the lethality of *BRC4*-induced cells (Fig. 7B). While both *BRCA2*$^{-/-}$ cells and *BRC4*-induced cells show defects in RAD51 foci formation ([15] and see Fig. 4B), the above phenotype clearly separates *BRCA2*$^{-/-}$ cells from *BRC4*-induced cells. We further confirmed the selectivity of BRC4 for RAD51 by using a BRC4 variant, BRC4-A1504S, deficient for RAD51 interaction [36]. Differently from *BRC4*, overexpression of *BRC4-A1504S* did not affect cell growth (Fig. 7C and D). These results, taken together with the ones above, substantiate the notion that the cytotoxicity associated with high levels of BRC4 arises specifically from its inhibitory binding to RAD51.

3.8. *BRC4* cytotoxicity is enhanced by DNA damaging agents, but counteracted by *RAD51* overexpression

RAD51 is essential for both cell survival and HR repair. Previous studies showed that *BRC4* expression induces hypersensitivity to γ-irradiation and DNA damaging agents such as CDDP [7,14]. We examined if, similarly to *RAD51* deficiency, *BRC4* induction would affect not only cell growth (Fig. 3) but also the cellular response to DNA damage. Because HR deficient mutants such as *BRCA2* or *RAD51* paralog knockout cells are highly sensitive to olaparib and camptothecin (CPT) [15,37], we incubated *BRC4* cells with either of these drugs in the presence or absence of Dox (Fig. 8A

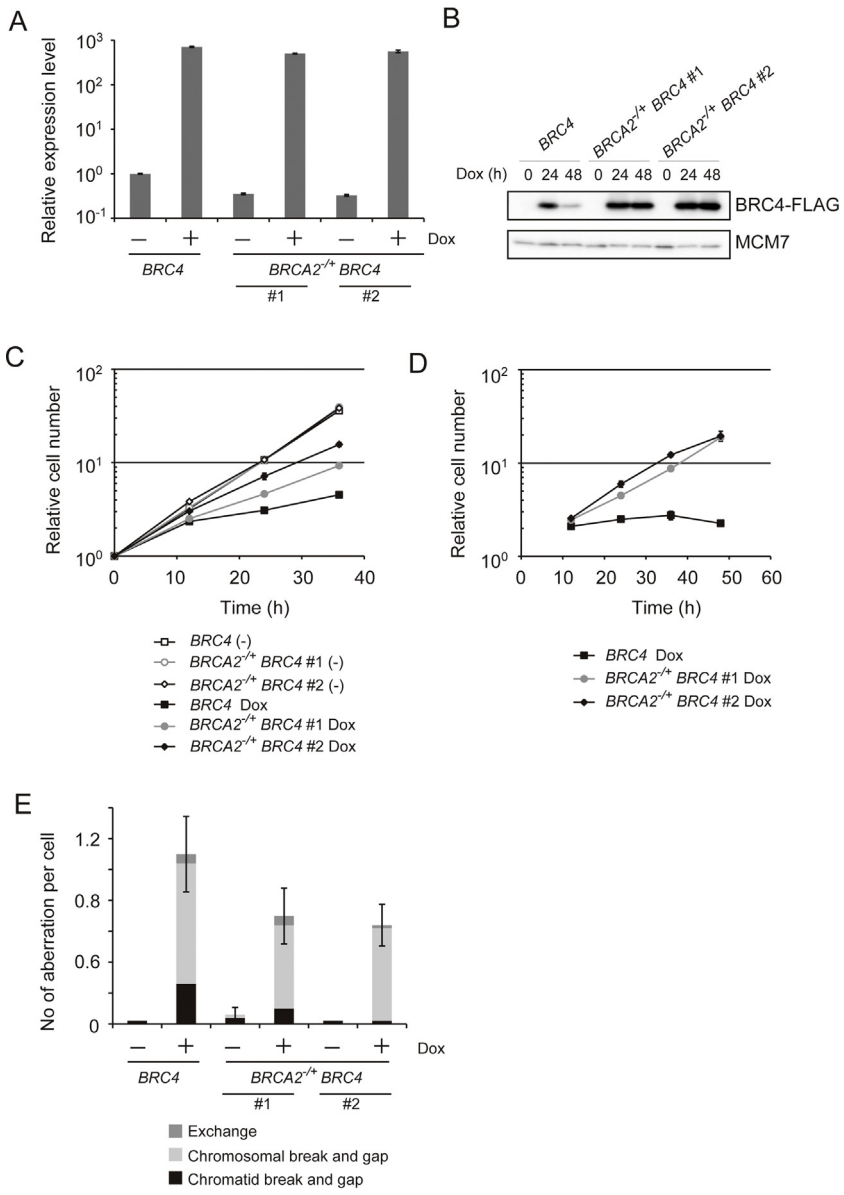

Fig. 5. BRC4 cytotoxicity depends on endogenous BRCA2. (A) Relative *BRC4* expression level measured by qPCR. *BRC4* cells and individually obtained 2 clones of *BRCA2*$^{-/+}$ *BRC4* cells were incubated in the presence or absence of Dox for 12 h and RNA was isolated. Isolated cDNA was used for qPCR. (B) Expression of BRC4–FLAG peptide. Whole cell lysates were prepared from each cell line cultured in the presence of Dox for the indicated times. BRC4–FLAG and MCM7 (loading control) were detected by Western blotting. (C) Growth curves. *BRC4* or individually obtained 2 clones of *BRCA2*$^{-/+}$ *BRC4* cells (1×10^5) were inoculated in 1 ml of medium and passaged every 12 h. Dox was added at time 0. (D) Growth curves of mCherry positive cells. The number of cells expressing mCherry was counted every 12 h. (E) Number of chromosomal aberrations in *BRC4* and *BRCA2*$^{-/+}$ *BRC4* cells after treatment with Dox for 24 h.

and B). We used low concentrations of drugs, 0.5 μM for olaparib and 5 nM for CPT, respectively, that do not impact on cell growth in WT cells. Indeed, *BRC4* cells showed normal growth in the absence of Dox, but *BRC4*-induced cells showed growth defects (see also Fig. 3C) that were exacerbated following treatment with low doses of these drugs (Fig. 8A and B). These results show that inhibition of RAD51 function by BRC4 not only induces chromosomal damage, but also inhibits DNA repair [7,14]. Because *RAD51* overexpression counteracted the cytotoxicity associated with *BRC4* induction (Fig. 7), we tested if it may also counteract the DNA repair defects of *BRC4*-induced cells. Differently from *XRCC3*$^{-/-}$ cells, used here as control because of their hypersensitivity to olaparib [37], *BRC4* cells overexpressing *RAD51* did not show high sensitivity to olaparib either in the absence or presence of Dox that induces *BRC4* (Fig. 8C). These results indicate that both the cytotoxicity and the DNA repair defects associated with *BRC4* induction are related to its inhibitory effect on RAD51 and can be overcome by increasing RAD51 amounts. These results thus suggest that HR is proficient in cells overexpressing both *BRC4* and *RAD51*. Surprisingly, bright RAD51 foci induced by MMC were abolished in cells overexpressing both *RAD51* and *BRC4*, whereas faint foci could still be observed (Fig. 8D and E). Collectively, these results indicate that BRC4 affects RAD51 polymerization even if *RAD51* is overexpressed in the cells, but that the small RAD51 factories assembled under these conditions are proficient in mediating HR-mediated DNA repair.

4. Discussion

Conditional expression systems are powerful tools to study the molecular mechanisms underlying the cytotoxicity associated with specific proteins. Though the expression of target proteins should

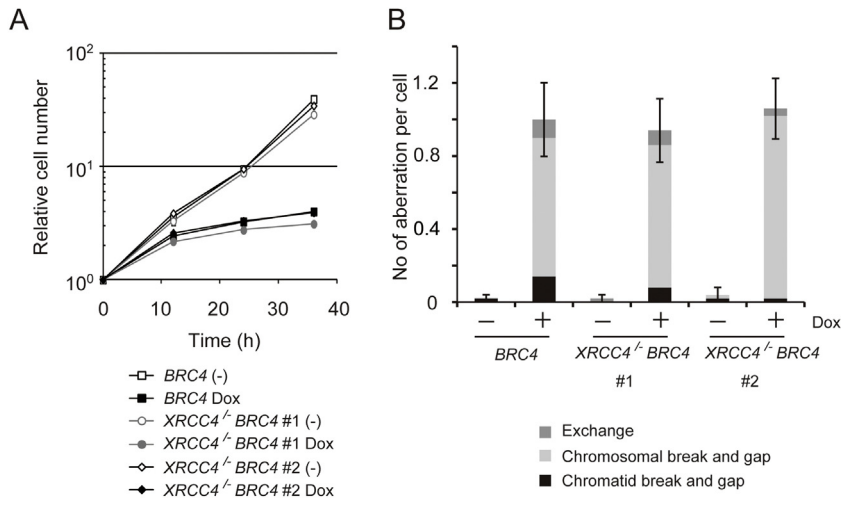

Fig. 6. BRC4-induced cytotoxicity is not dependent on non-homologous end joining. (A) Growth curves. *BRC4* and individually obtained 2 clones of *XRCC4/*$^{-}$ *BRC4* cells (1×10^5) were inoculated in 1 ml of medium and passaged every 12 h. Dox was added at time labeled 0. (B) Number of chromosomal aberrations in *BRC4* and *XRCC4/*$^{-}$ *BRC4* cells after treatment with Dox for 24 h.

be completely repressed in 'off state', old Tet-On systems suffered of leaky expression problems. In this study, we applied the newly developed Tet-On 3G system to chicken DT40 cells to study three proteins. The expression of *p53*, I-*Sce*I and *BRC4* analyzed here was completely repressed in the absence of Dox, whereas Dox addition induced expressions of these genes, thus establishing the Tet-On 3G system as suitable in DT40 research. Analysis of the phenotypes associated with specific gene inductions also revealed novel aspects on the mode of action of these proteins, particularly on the mode of action of BRC4 and BRCA2, which are discussed below.

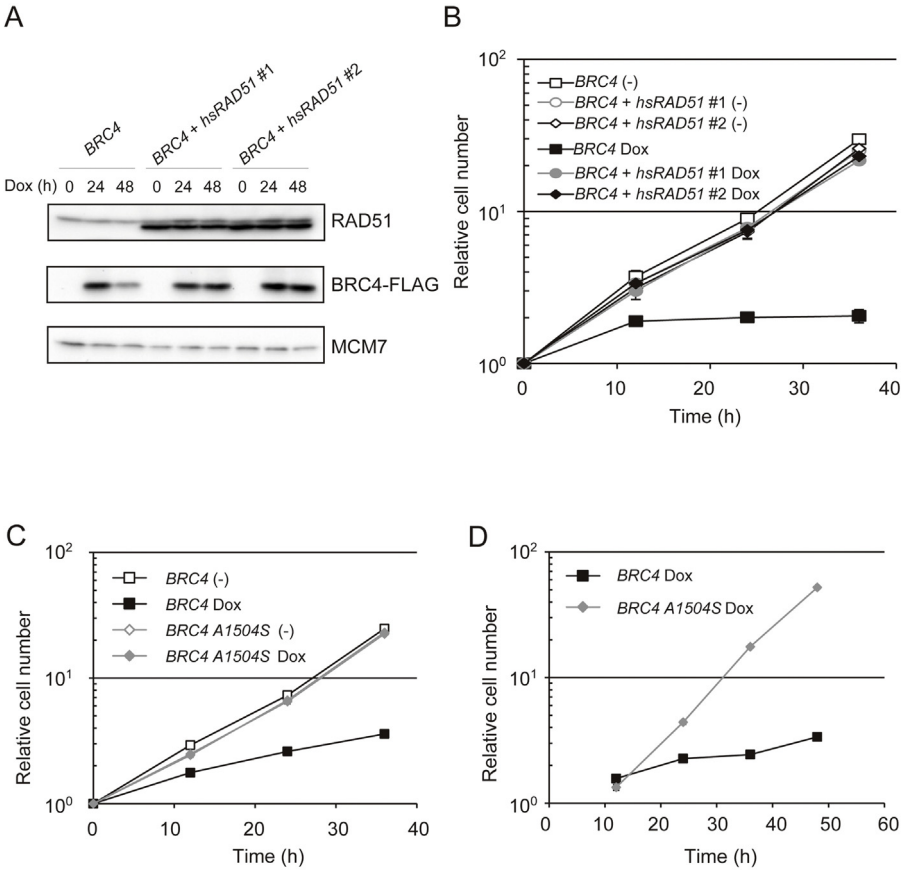

Fig. 7. *RAD51* overexpression rescues *BRC4*-induced cytotoxicity. (A) Expression of RAD51 and BRC4–FLAG peptide. Whole cell lysates were prepared from each cell lines cultured in the presence of Dox for the indicated times. RAD51, BRC4–FLAG and MCM7 (loading control) were detected by Western blotting. The upper and lower bands of RAD51 show chicken and human RAD51, respectively. (B) Growth curves. *BRC4* and individually obtained 2 clones of *BRC4* + *hsRAD51* cells (1×10^5) were inoculated in 1 ml of medium and passaged every 12 h. Dox was added at the time point labeled 0. (C) Growth curves of *BRC4* and *BRC4-A1504S* cells in the presence or absence of Dox. 1×10^5 cells of the indicated genotype were inoculated in 1 ml of medium and passaged every 12 h. Dox was added at time 0. (D) Growth curves of mCherry positive *BRC4* and *BRC4-A1504S* cells. The number of cells expressing mCherry was counted every 12 h.

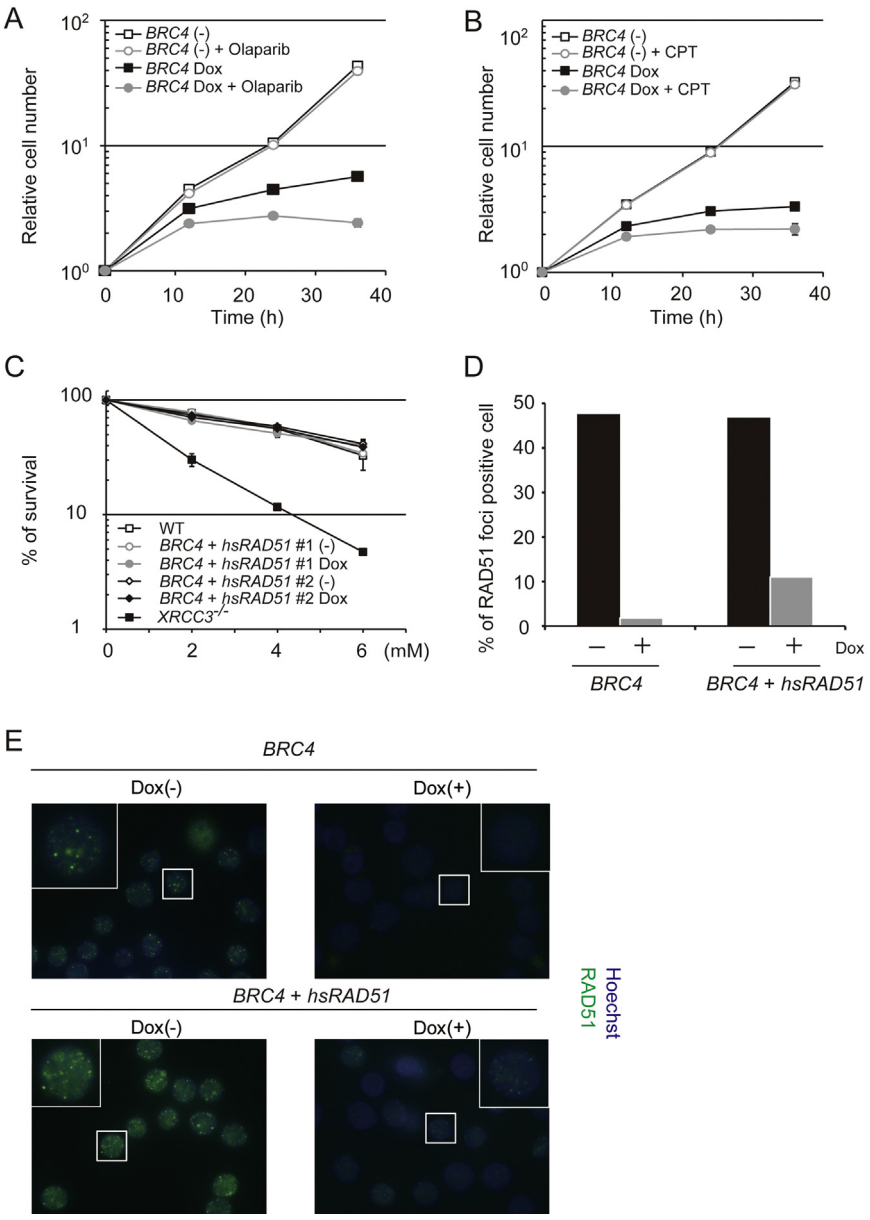

Fig. 8. *Rad51* overexpression rescues *BRC4*-induced homologous recombination repair defects. (A) and (B) growth curves. *BRC4* cells (1×10^5) were inoculated in 1 ml of medium and passaged every 12 h. Dox and olaparib (A) or CPT (B) were added at time 0. (C) Sensitivity of indicated cells to olaparib. Dox was added 24 h before the experiment. Cell survival percentage is displayed as the ratio of the number of surviving cells following olaparib treatment relative to the untreated control. Each line and error bar represents the mean value and SD from three independent experiments, respectively. (D) and (E) Rad51 focus formation. *BRC4* cells and *BRC4* + *hsRAD51* cells were incubated in the presence or absence of Dox for 20 h. Then cells were exposed to 500 ng/ml of MMC for 6 h. Cytoplasmic RAD51 was washed out by pre-triton treatment prior to fixation to reduce the background. At least 100 cells were scored for each preparation. Identical trends were observed in independently conducted experiments.

High levels of BRC4 induced cell lethality and chromosomal type breaks, reminiscent of the cytotoxicity associated with radiation or RAD51 deficiencies (Fig. 3). Although none of the past studies using BRC4 or other Brc repeats reported their cytotoxicity [7,8,14], the difference between the past studies and ours likely comes from the expression levels of *BRC4* as in our system high amounts of *BRC4* were induced (Fig. 3A). Another possible reason for this new phenotype revealed here may be due to species differences and related changes of critical residues within the BRC repeats that impact on the strength of the BRC4–Rad51 interaction [38]. One of these examples is the V1532 residue of the BRC4 repeat of human BRCA2, which is substituted by isoleucine in canine species as well as in chicken BRCA2 [27]. In this vein, a recent study reported enhanced binding of human BRC4 to RAD51 as well as RAD51–DNA dissociation activity by replacing several amino acids of BRC4 [36].

The cytotoxic effect of BRC4 was further enhanced by the addition of low concentrations of olaparib and CPT (Fig. 8A and B), indicating that BRC4 not only induces chromosomal breaks (Fig. 3E) but that it also inhibits DNA repair simultaneously. The cytotoxicity and inhibition of DNA repair by BRC4 completely depended on RAD51 (Figs. 7 and 8). These results indicate that the target of BRC4 in cells is RAD51 and that BRC4 blocks RAD51 polymerization in a competitive manner, together with endogenous BRCA2, likely in a fashion that depends on the presence of other BRC repeats or C-terminal residues of BRCA2 (Fig. 5). Alternatively, the effect of *BRC4* induction may be dependent on the endogenous *BRC4* repeat. In this regard, we note that although the level of *BRC4* mRNA induced by

the Tet-On 3G system was much higher than that of endogenous *BRCA2* mRNA, the stability of the BRC4 peptide may be lower than that of BRCA2. Further studies will be required to examine whether full length BRCA2 also inhibits RAD51 polymerization when overexpressed and to clarify a possible interplay between BRC4 and other BRCA2 domains in inhibiting RAD51-mediated DNA repair.

On the other hand, the interplay between BRC4 and BRCA2 in mediating cytotoxicity might reflect that distinct BRC repeats have separate activities in controlling genome integrity. Thus, while BRC4 plays a prominent role in regulating recombination repair, other BRC repeats may be involved in controlling mitotic cell cycle arrest, as it has been recently suggested for the BRC5 repeat of human BRCA2 [39]. While the BRC5 repeat itself is not conserved in chicken BRCA2, it is possible that analogous mechanisms exist, or that other BRC repeats of chicken BRCA2 substitute for human BRC5 in what regards the interaction with factors implicated in cell division. The finding that *BRC4* overexpression induces both lesions and ATM-mediated cell-cycle arrest (Fig. 3) does not exclude this view, but other explanations remain possible. For instance, BRC4 and other domains of BRCA2 may coordinately modulate DNA repair, either by similar or divergent roles. Interestingly, our results indicate that NHEJ is not involved in processing BRC4-induced DNA damage (Fig. 6), even in the absence of proper HR function. While this could simply reflect a cell cycle-mediated down-regulation of NHEJ in G2, similarly to what has been reported in yeast [40–42], it is also possible that other BRC repeats or domains of BRCA2 play a role in suppressing alternative error-prone repair mechanisms, such as NHEJ, thus explaining the tumor suppressor function of BRCA2.

In addition to shedding new light on the BRCA2 and BRC4 function *in vivo*, the results of this study indicate that BRC4 is proficient at killing proliferating cancer cells as well as enhancing the cytotoxic effects of olaparib and CPT (Fig. 8A and B) in a manner completely dependent on its inhibitory activity on RAD51. These features of BRC4 may be useful as a molecularly-targeted adjunctive agent to enhance the effect of other anti-cancer drugs. It is of note that over 35% of breast, ovarian and prostate carcinoma associated with germline *BRCA* mutations do not respond to olaparib [43] nor do the sporadic breast cancers not associated with *BRCA* mutations. It is likely that (concomitant) inhibition of RAD51 function in tumors that depend on HR for viability would lead to improved drug therapy. Although there is a considerable barrier to efficiently deliver peptide medicines to the focus of disease in patients, developments in drug delivery systems may make such peptide medications feasible in the future. Several specific RAD51 inhibitors have been reported recently [44–46]. Although it is still unknown if similarly to BRC4 these reagents specifically inhibit RAD51, together with BRC4 peptides, they constitute attractive anti-cancer drug candidates and useful *in vitro* tools to study the interplay between different repair pathways and their impact on genome integrity.

Conflict of interest statement

The authors declare that there are no conflicts of interest.

- Takuya Abe is in the
- *IFOM, The FIRC Institute for Molecular Oncology Foundation, IFOM-IEO Campus, Via Adamello 16, 20139 Milan, Italy.* Tel.: +39 02 574 303 259; e-mail: takuya.abe@ifom.eu.
- Dana Branzei is in the
- *IFOM, The FIRC Institute for Molecular Oncology Foundation, IFOM-IEO Campus, Via Adamello 16, 20139 Milan, Italy.* Tel.: +39 02 574 303 259; e-mail: dana.branzei@ifom.eu.

Acknowledgements

We thank Dr. S. Takeda (Kyoto University) for the gifts of *BRCA2*$^{-/+}$, *XRCC3*$^{-/-}$, *RAD51*$^{-/-}$ + *hsRAD51* cells and DR-GFP/chicken *OVA* targeting construct, Dr. H. Arakawa (IFOM) for helpful discussions, and Dr. H. Kajiho (IFOM) for technical advice on microscope experiments. This work was supported by the European Research Council [REPSUBREP 242928]; the Italian Association for Cancer Research [AIRC IG grant 10637]; Fondazione Telethon [grant GGP12160]; and FIRC. T. Abe was partly supported by the Structured International Post Doc Program (SIPOD) fellowship co-funded in the context of the FP7 Marie Curie Actions—People.

Appendix A. Supplementary data

Supplementary data associated with this article can be found, in the online version, at http://dx.doi.org/10.1016/j.dnarep.2014.08.003.

References

[1] M.E. Moynahan, M. Jasin, Mitotic homologous recombination maintains genomic stability and suppresses tumorigenesis, Nat. Rev. Mol. Cell Biol. 11 (2010) 196–207.
[2] H.L. Klein, The consequences of Rad51 overexpression for normal and tumor cells, DNA Repair (Amst.) 7 (2008) 686–693.
[3] L. Costantino, S.K. Sotiriou, J.K. Rantala, S. Magin, E. Mladenov, T. Helleday, J.E. Haber, G. Iliakis, O.P. Kallioniemi, T.D. Halazonetis, Break-induced replication repair of damaged forks induces genomic duplications in human cells, Science 343 (2014) 88–91.
[4] A.R. Venkitaraman, Chromosome stability, DNA recombination and the BRCA2 tumour suppressor, Curr. Opin. Cell Biol. 13 (2001) 338–343.
[5] A.K. Wong, R. Pero, P.A. Ormonde, S.V. Tavtigian, P.L. Bartel, RAD51 interacts with the evolutionarily conserved BRC motifs in the human breast cancer susceptibility gene BRCA2, J. Biol. Chem. 272 (1997) 31941–31944.
[6] A.A. Davies, J.Y. Masson, M.J. McIlwraith, A.Z. Stasiak, A. Stasiak, A.R. Venkitaraman, S.C. West, Role of BRCA2 in control of the RAD51 recombination and DNA repair protein, Mol. Cell 7 (2001) 273–282.
[7] C.F. Chen, P.L. Chen, Q. Zhong, Z.D. Sharp, W.H. Lee, Expression of BRC repeats in breast cancer cells disrupts the BRCA2–Rad51 complex and leads to radiation hypersensitivity and loss of G(2)/M checkpoint control, J. Biol. Chem. 274 (1999) 32931–32935.
[8] L. Pellegrini, D.S. Yu, T. Lo, S. Anand, M. Lee, T.L. Blundell, A.R. Venkitaraman, Insights into DNA recombination from the structure of a RAD51–BRCA2 complex, Nature 420 (2002) 287–293.
[9] P. Bork, N. Blomberg, M. Nilges, Internal repeats in the BRCA2 protein sequence, Nat. Genet. 13 (1996) 22–23.
[10] A. Carreira, J. Hilario, I. Amitani, R.J. Baskin, M.K. Shivji, A.R. Venkitaraman, S.C. Kowalczykowski, The BRC repeats of BRCA2 modulate the DNA-binding selectivity of RAD51, Cell 136 (2009) 1032–1043.
[11] J. Nomme, Y. Takizawa, S.F. Martinez, A. Renodon-Corniere, F. Fleury, P. Weigel, K. Yamamoto, H. Kurumizaka, M. Takahashi, Inhibition of filament formation of human Rad51 protein by a small peptide derived from the BRC-motif of the BRCA2 protein, Genes Cells 13 (2008) 471–481.
[12] V.E. Galkin, F. Esashi, X. Yu, S. Yang, S.C. West, E.H. Egelman, BRCA2 BRC motifs bind RAD51–DNA filaments, Proc. Natl. Acad. Sci. U.S.A. 102 (2005) 8537–8542.
[13] M.K. Shivji, O.R. Davies, J.M. Savill, D.L. Bates, L. Pellegrini, A.R. Venkitaraman, A region of human BRCA2 containing multiple BRC repeats promotes RAD51-mediated strand exchange, Nucleic Acids Res. 34 (2006) 4000–4011.
[14] S.S. Yuan, S.Y. Lee, G. Chen, M. Song, G.E. Tomlinson, E.Y. Lee, BRCA2 is required for ionizing radiation-induced assembly of Rad51 complex in vivo, Cancer Res. 59 (1999) 3547–3551.
[15] Y. Qing, M. Yamazoe, K. Hirota, D. Dejsuphong, W. Sakai, K.N. Yamamoto, D.K. Bishop, X. Wu, S. Takeda, The epistatic relationship between BRCA2 and the other RAD51 mediators in homologous recombination, PLoS Genet. 7 (2011) e1002148.
[16] J.M. Buerstedde, S. Takeda, Increased ratio of targeted to random integration after transfection of chicken B cell lines, Cell 67 (1991) 179–188.
[17] M. Takata, M.S. Sasaki, S. Tachiiri, T. Fukushima, E. Sonoda, D. Schild, L.H. Thompson, S. Takeda, Chromosome instability and defective recombinational repair in knockout mutants of the five Rad51 paralogs, Mol. Cell Biol. 21 (2001) 2858–2866.
[18] E. Sonoda, M.S. Sasaki, J.M. Buerstedde, O. Bezzubova, A. Shinohara, H. Ogawa, M. Takata, Y. Yamaguchi-Iwai, S. Takeda, Rad51-deficient vertebrate cells accumulate chromosomal breaks prior to cell death, EMBO J. 17 (1998) 598–608.
[19] T. Abe, M. Ishiai, Y. Hosono, A. Yoshimura, S. Tada, N. Adachi, H. Koyama, M. Takata, S. Takeda, T. Enomoto, M. Seki, KU70/80, DNA-PKcs, and Artemis are essential for the rapid induction of apoptosis after massive DSB formation, Cell. Signal. 20 (2008) 1978–1985.

[20] R. Loew, N. Heinz, M. Hampf, H. Bujard, M. Gossen, Improved Tet-responsive promoters with minimized background expression, BMC Biotechnol. 10 (2010) 81.
[21] X. Zhou, M. Vink, B. Klaver, B. Berkhout, A.T. Das, Optimization of the Tet-On system for regulated gene expression through viral evolution, Gene Ther. 13 (2006) 1382–1390.
[22] N. Takao, Y. Li, K. Yamamoto, Protective roles for ATM in cellular response to oxidative stress, FEBS Lett. 472 (2000) 133–136.
[23] A.J. Levine, p53, the cellular gatekeeper for growth and division, Cell 88 (1997) 323–331.
[24] X. Wang, K. Takenaka, S. Takeda, PTIP promotes DNA double-strand break repair through homologous recombination, Genes Cells 15 (2010) 243–254.
[25] T. Fukushima, M. Takata, C. Morrison, R. Araki, A. Fujimori, M. Abe, K. Tatsumi, M. Jasin, P.K. Dhar, E. Sonoda, T. Chiba, S. Takeda, Genetic analysis of the DNA-dependent protein kinase reveals an inhibitory role of Ku in late S-G2 phase DNA double-strand break repair, J. Biol. Chem. 276 (2001) 44413–44418.
[26] B.L. Mahaney, K. Meek, S.P. Lees-Miller, Repair of ionizing radiation-induced DNA double-strand breaks by non-homologous end-joining, Biochem. J. 417 (2009) 639–650.
[27] M. Takata, S. Tachiiri, A. Fujimori, L.H. Thompson, Y. Miki, M. Hiraoka, S. Takeda, M. Yamazoe, Conserved domains in the chicken homologue of BRCA2, Oncogene 21 (2002) 1130–1134.
[28] D.S. Lim, P. Hasty, A mutation in mouse rad51 results in an early embryonic lethal that is suppressed by a mutation in p53, Mol. Cell Biol. 16 (1996) 7133–7143.
[29] S. Burma, B.P. Chen, M. Murphy, A. Kurimasa, D.J. Chen, ATM phosphorylates histone H2AX in response to DNA double-strand breaks, J. Biol. Chem. 276 (2001) 42462–42467.
[30] M.I. Petalcorin, V.E. Galkin, X. Yu, E.H. Egelman, S.J. Boulton, Stabilization of RAD-51–DNA filaments via an interaction domain in *Caenorhabditis elegans* BRCA2, Proc. Natl. Acad. Sci. U.S.A. 104 (2007) 8299–8304.
[31] O.R. Davies, L. Pellegrini, Interaction with the BRCA2 C terminus protects RAD51–DNA filaments from disassembly by BRC repeats, Nat. Struct. Mol. Biol. 14 (2007) 475–483.
[32] F. Esashi, V.E. Galkin, X. Yu, E.H. Egelman, S.C. West, Stabilization of RAD51 nucleoprotein filaments by the C-terminal region of BRCA2, Nat. Struct. Mol. Biol. 14 (2007) 468–474.
[33] J.T. Holthausen, M.T. van Loenhout, H. Sanchez, D. Ristic, S.E. van Rossum-Fikkert, M. Modesti, C. Dekker, R. Kanaar, C. Wyman, Effect of the BRCA2 CTRD domain on RAD51 filaments analyzed by an ensemble of single molecule techniques, Nucleic Acids Res. 39 (2011) 6558–6567.
[34] R.W. Martin, B.J. Orelli, M. Yamazoe, A.J. Minn, S. Takeda, D.K. Bishop, RAD51 up-regulation bypasses BRCA1 function and is a common feature of BRCA1-deficient breast tumors, Cancer Res. 67 (2007) 9658–9665.
[35] A. Hatanaka, M. Yamazoe, J.E. Sale, M. Takata, K. Yamamoto, H. Kitao, E. Sonoda, K. Kikuchi, Y. Yonetani, S. Takeda, Similar effects of Brca2 truncation and Rad51 paralog deficiency on immunoglobulin V gene diversification in DT40 cells support an early role for Rad51 paralogs in homologous recombination, Mol. Cell Biol. 25 (2005) 1124–1134.
[36] J. Nomme, A. Renodon-Corniere, Y. Asanomi, K. Sakaguchi, A.Z. Stasiak, A. Stasiak, B. Norden, V. Tran, M. Takahashi, Design of potent inhibitors of human RAD51 recombinase based on BRC motifs of BRCA2 protein: modeling and experimental validation of a chimera peptide, J. Med. Chem. 53 (2010) 5782–5791.
[37] J. Murai, S.Y. Huang, B.B. Das, A. Renaud, Y. Zhang, J.H. Doroshow, J. Ji, S. Takeda, Y. Pommier, Trapping of PARP1 and PARP2 by Clinical PARP Inhibitors, Cancer Res. 72 (2012) 5588–5599.
[38] K. Ochiai, Y. Yoshikawa, K. Yoshimatsu, T. Oonuma, Y. Tomioka, E. Takeda, J. Arikawa, K. Mominoki, T. Omi, K. Hashizume, M. Morimatsu, Valine 1532 of human BRC repeat 4 plays an important role in the interaction between BRCA2 and RAD51, FEBS Lett. 585 (2011) 1771–1777.
[39] M. Lee, M.J. Daniels, M.J. Garnett, A.R. Venkitaraman, A mitotic function for the high-mobility group protein HMG20b regulated by its interaction with the BRC repeats of the BRCA2 tumor suppressor, Oncogene 30 (2011) 3360–3369.
[40] L.S. Symington, J. Gautier, Double-strand break end resection and repair pathway choice, Annu. Rev. Genet. 45 (2011) 247–271.
[41] Y. Zhang, E.Y. Shim, M. Davis, S.E. Lee, Regulation of repair choice: Cdk1 suppresses recruitment of end joining factors at DNA breaks, DNA Repair (Amst.) 8 (2009) 1235–1241.
[42] G. Ira, A. Pellicioli, A. Balijja, X. Wang, S. Fiorani, W. Carotenuto, G. Liberi, D. Bressan, L. Wan, N.M. Hollingsworth, J.E. Haber, M. Foiani, DNA end resection, homologous recombination and DNA damage checkpoint activation require CDK1, Nature 431 (2004) 1011–1017.
[43] P.C. Fong, D.S. Boss, T.A. Yap, A. Tutt, P. Wu, M. Mergui-Roelvink, P. Mortimer, H. Swaisland, A. Lau, M.J. O'Connor, A. Ashworth, J. Carmichael, S.B. Kaye, J.H. Schellens, J.S. de Bono, Inhibition of poly(ADP-ribose) polymerase in tumors from BRCA mutation carriers, N. Engl. J. Med. 361 (2009) 123–134.
[44] J. Zhu, L. Zhou, G. Wu, H. Konig, X. Lin, G. Li, X.L. Qiu, C.F. Chen, C.M. Hu, E. Goldblatt, R. Bhatia, A.R. Chamberlin, P.L. Chen, W.H. Lee, A novel small molecule RAD51 inactivator overcomes imatinib-resistance in chronic myeloid leukaemia, EMBO Mol. Med. 5 (2013) 353–365.
[45] D.E. Scott, M.T. Ehebauer, T. Pukala, M. Marsh, T.L. Blundell, A.R. Venkitaraman, C. Abell, M. Hyvonen, Using a fragment-based approach to target protein-protein interactions, ChemBioChem 14 (2013) 332–342.
[46] B. Budke, J.H. Kalin, M. Pawlowski, A.S. Zelivianskaia, M. Wu, A.P. Kozikowski, P.P. Connell, An optimized RAD51 inhibitor that disrupts homologous recombination without requiring Michael acceptor reactivity, J. Med. Chem. 56 (2013) 254–263.